The Mitochondrial Sulfur Dioxygenase ETHYLMALONIC ENCEPHALOPATHY PROTEIN1 Is Required for Amino Acid Catabolism during Carbohydrate Starvation and Embryo Development in Arabidopsis[1][C][W]

Lena Krüßel, Johannes Junemann, Markus Wirtz, Hannah Birke[2], Jeremy D. Thornton, Luke W. Browning, Gernot Poschet, Rüdiger Hell, Janneke Balk, Hans-Peter Braun, and Tatjana M. Hildebrandt*

Institute for Plant Genetics, Leibniz University Hannover, 30419 Hannover, Germany (L.K., J.J., H.-P.B., T.M.H.); Centre for Organismal Studies Heidelberg (M.W., H.B., R.H.) and Metabolomics Core Technology Platform Heidelberg (G.P., R.H.), University of Heidelberg, 69120 Heidelberg, Germany; John Innes Centre, Norwich NR4 7UH, United Kingdom (J.D.T., L.W.B., J.B.); and School of Biological Sciences, University of East Anglia, Norwich NR4 7JT, United Kingdom (J.D.T., L.W.B., J.B.)

The sulfur dioxygenase ETHYLMALONIC ENCEPHALOPATHY PROTEIN1 (ETHE1) catalyzes the oxidation of persulfides in the mitochondrial matrix and is essential for early embryo development in Arabidopsis (*Arabidopsis thaliana*). We investigated the biochemical and physiological functions of ETHE1 in plant metabolism using recombinant Arabidopsis ETHE1 and three transfer DNA insertion lines with 50% to 99% decreased sulfur dioxygenase activity. Our results identified a new mitochondrial pathway catalyzing the detoxification of reduced sulfur species derived from cysteine catabolism by oxidation to thiosulfate. Knockdown of the sulfur dioxygenase impaired embryo development and produced phenotypes of starvation-induced chlorosis during short-day growth conditions and extended darkness, indicating that ETHE1 has a key function in situations of high protein turnover, such as seed production and the use of amino acids as alternative respiratory substrates during carbohydrate starvation. The amino acid profile of mutant plants was similar to that caused by defects in the electron-transfer flavoprotein/electron-transfer flavoprotein: ubiquinone oxidoreductase complex and associated dehydrogenases. Thus, in addition to sulfur amino acid catabolism, ETHE1 also affects the oxidation of branched-chain amino acids and lysine.

Protein recycling is involved in many cellular processes, including metabolic regulation and programmed cell death. Damaged or dispensable proteins and entire organelles are degraded to provide carbohydrates and nitrogen for energy production and the synthesis of new material. In plants, this turnover is essential for tissue remodeling during senescence and seed production as well as for survival under nutrient-limiting stress conditions (Li and Vierstra, 2012). Catabolism of the sulfur-containing amino acids Cys and Met is still largely unknown. Several enzymes have been shown to release sulfur from Cys. L-Cys desulfurases (nitrogen fixation1 homolog [*Saccharomyces cerevisiae*; NFS1] and NFS2; EC 2.8.1.7) provide persulfide for the biosynthesis of iron-sulfur clusters, thiamine, biotin, and molybdenum cofactor (van Hoewyk et al., 2008; Balk and Pilon, 2011). β-Cyanoalanine synthase (EC 4.4.1.9) detoxifies cyanide under the consumption of Cys and releases β-cyanoalanine and sulfide (Hatzfeld et al., 2000). Cytosolic L-Cys desulfhydrase (DES1; EC 4.4.1.1) and mitochondrial D-Cys desulfhydrase (EC 4.4.1.15) catalyze β-elimination reactions of L- or D-Cys to pyruvate, ammonium, and hydrogen sulfide (H_2S; Riemenschneider et al., 2005; Alvarez et al., 2010). Since their expression increases with age, Cys desulfhydrases have been suggested to be involved in the catabolism of sulfur-containing amino acids during senescence (Riemenschneider et al., 2005; Jin et al., 2011).

Recently, several regulatory functions of sulfide in plants have emerged. Sulfide increases drought resistance by inducing stomatal closure (García-Mata and Lamattina 2010; Jin et al., 2011, 2013) and is also protective against other abiotic stresses such as heat and heavy metals (Zhang et al., 2008, 2010; Li et al., 2012). It negatively

[1] This work was supported by the Deutsche Forschungsgemeinschaft (grant no. HI 1471/1–1 to T.M.H. and grant no. ZUK 40/2010–3009262).

[2] Present address: Commonwealth Scientific and Industrial Research Organization Plant Industry, Black Mountain Laboratories, Canberra, ACT 2601, Australia.

* Address correspondence to hildebrandt@genetik.uni-hannover.de.

The author responsible for distribution of materials integral to the findings presented in this article in accordance with the policy described in the Instructions for Authors (www.plantphysiol.org) is: Tatjana M. Hildebrandt (hildebrandt@genetik.uni-hannover.de).

[C] Some figures in this article are displayed in color online but in black and white in the print edition.

[W] The online version of this article contains Web-only data.

www.plantphysiol.org/cgi/doi/10.1104/pp.114.239764

regulates autophagy and is probably involved in several additional aspects of plant development (Álvarez et al., 2012; Dooley et al., 2013). However, sulfide is also a potent inhibitor of cytochrome *c* oxidase (COX) and negatively affects plant growth (Birke et al., 2012), making efficient removal of excess sulfide essential for the survival of the plant. Although fixation of sulfide into Cys contributes substantially to sulfide detoxification, the presence of an additional, so far unknown mechanism in mitochondria was revealed but not further analyzed (Birke et al., 2012).

ETHYLMALONIC ENCEPHALOPATHY PROTEIN1 (ETHE1) is a sulfur dioxygenase (SDO; EC 1.13.11.18) that oxidizes persulfides in the mitochondrial matrix and, therefore, constitutes a good candidate to be involved in plant sulfur catabolism. In Arabidopsis (*Arabidopsis thaliana*), ETHE1 (AT1G53580) is critical for seed production. A loss-of-function mutation causes alterations in the mitochondrial ultrastructure and an arrest of embryo development at early heart stage (Holdorf et al., 2012). However, the precise biochemical and physiological roles of ETHE1 in plant mitochondria have not been established. Mutations in the human homolog ETHE1 lead to the fatal metabolic disease ethylmalonic encephalopathy (Tiranti et al., 2004). The primary cause for the disease is a disruption of the mitochondrial sulfide detoxification pathway that oxidizes sulfide to either thiosulfate or sulfate in four steps catalyzed by sulfide:quinone oxidoreductase, ETHE1, a sulfurtransferase, and sulfite oxidase (Hildebrandt and Grieshaber, 2008; Tiranti et al., 2009). Increased sulfide concentrations in the bloodstream severely damage the vascular endothelium and thus cause the main symptoms of ethylmalonic encephalopathy: rapidly progressive necrosis in the brain, chronic diarrhea, and microangiopathy (Giordano et al., 2012). In addition, sulfide interferes with mitochondrial energy metabolism. It reversibly inhibits COX at low micromolar concentrations (Tiranti et al., 2009), and chronic exposure destabilizes specific COX subunits (Di Meo et al., 2011). ETHE1 deficiency also affects the mitochondrial catabolism of fatty acids and branched-chain amino acids (BCAA), leading to an accumulation of ethylmalonic acid as well as C4 and C5 acylcarnitines and acylglycines (Tiranti et al., 2009; Hildebrandt et al., 2013).

Here, we show that in Arabidopsis, the mitochondrial SDO ETHE1 is part of a sulfur catabolic pathway that catalyzes the oxidation of sulfide or persulfides derived from amino acids to thiosulfate and sulfate. ETHE1 has a key function in situations of high protein turnover, such as seed production or unfavorable environmental conditions leading to carbohydrate starvation and the use of amino acids as alternative respiratory substrates.

RESULTS

We analyzed three transfer DNA (T-DNA) insertion lines of the *AT1G53580* gene to investigate the physiological function of ETHE1 in Arabidopsis. In the mutant line *ethe1-1*, the T-DNA is inserted into the 5′ untranslated region 64 bp upstream of the start codon (Fig. 1A), leading to a decrease in *ETHE1* transcript level by 75% (Fig. 1B). Immunolabeling showed that only trace amounts of ETHE1 protein were present in purified mitochondria of this line (Fig. 1C). In *ethe1-2* and *ethe1-3*, the T-DNA insertion is localized in the promoter region of the gene (335 and 327 bp upstream of the start codon; Fig. 1A). The *ETHE1* transcript level was 60% to 70% of the wild type, and ETHE1 protein abundance was also decreased in these lines (Fig. 1, B and C).

SDO activity was measured as oxygen consumption upon the addition of 1 mM reduced glutathione (GSH) and elemental sulfur using a Clarke-type oxygen electrode. The elemental sulfur rings react with GSH nonenzymatically to form polysulfane compounds including glutathione persulfide (GSSH), the substrate of the SDO reaction (Rohwerder and Sand, 2003). Mitochondria isolated from wild-type Arabidopsis cell suspension culture had an SDO activity of 36.0 ± 8.4 nmol oxygen min^{-1} mg^{-1} protein under standard conditions, which was comparable to the SDO activity in mitochondria isolated from wild-type rosette leaves (44.2 ± 2.7 nmol oxygen min^{-1} mg^{-1} protein; $n = 3$). By contrast, almost no SDO activity was detectable in mitochondria from the *ethe1-1* line, and the activity was decreased by 24% and 64% in *ethe1-2* and *ethe1-3*, respectively (Fig. 1D).

The *ETHE1* gene excluding the mitochondrial targeting sequence was expressed in *Escherichia coli* and purified using a C-terminal 6× His tag. Recombinant Arabidopsis ETHE1 protein had a specific activity of 35.3 ± 1.8 μmol oxygen min^{-1} mg^{-1} protein in the standard activity test for SDO, which is 1,000 times higher than that in isolated mitochondria. The pH optimum of Arabidopsis ETHE1 was around pH 9.0 and the temperature optimum was 55°C, compared with pH 7.5 and 35°C for human ETHE1 (Supplemental Fig. 1, B and C). These results confirm that ETHE1 in Arabidopsis is an SDO (EC 1.13.11.18).

ETHE1 Oxidizes GSSH to Sulfite

Recombinant Arabidopsis ETHE1 was highly specific for GSSH as a substrate. SDO activity comparable to the standard assay using GSH and elemental sulfur as a substrate was only observed in the presence of oxidized glutathione (GSSG) and sulfide, which also form GSSH in a nonenzymatic reaction (Fig. 2A). Free sulfide and 3-mercaptopyruvate were not oxidized, and GSH could not be replaced by other thiols such as Cys, 3-mercaptoethanol, and dithiothreitol (Supplemental Table S1).

Human ETHE1 is known to catalyze the reaction GSSH + oxygen + water → GSH + sulfite + $2H^+$ (Kabil and Banerjee, 2012). To confirm that sulfite is also the product of ETHE1 in Arabidopsis, we measured thiol levels during the course of the SDO activity assay (Fig. 2B). Sulfite was only detected after the addition of elemental sulfur and increased proportionately to the oxygen consumed. The total amount of sulfite produced, which was limited by 250 nmol of oxygen available in the electrode chamber, was 218 ± 42.4 nmol

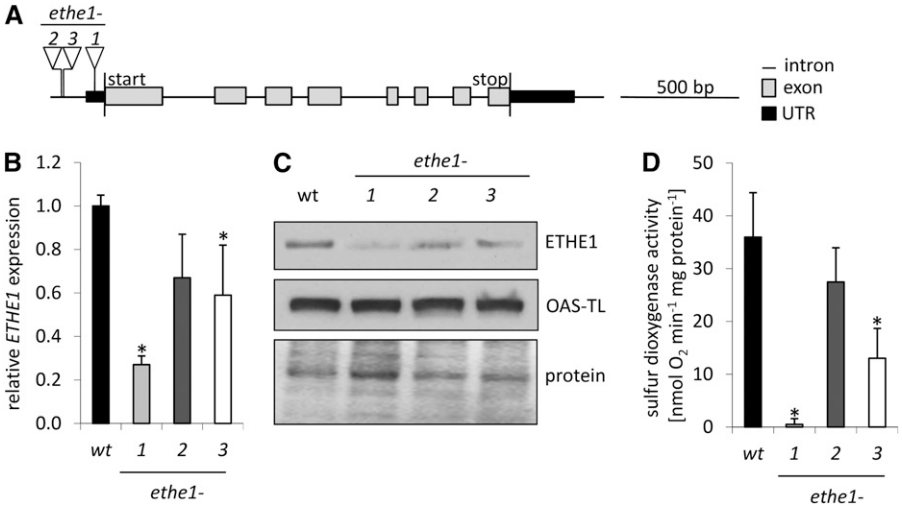

Figure 1. Molecular characterization of the T-DNA insertion lines *ethe1-1*, *ethe1-2*, and *ethe1-3*. A, Genomic structure of the *ETHE1* gene and positions of T-DNA insertions in the mutant lines (white triangles). UTR, Untranslated region. B, *ETHE1* expression in *ethe1* mutants was quantified relative to the wild type (wt) by quantitative RT-PCR ($n = 5$). Cytosolic *GAPDH* (AT1G13440) was used for normalization. C, Immunological detection of ETHE1 protein in mitochondria isolated from cell suspension cultures of the wild type and the *ethe1* mutants. Purity of the mitochondrial fraction was confirmed using an OAS (thiol) lyase (OAS-TL) antibody. This antibody recognizes OAS (thiol) lyase isoforms localized in the mitochondria, the plastids, and the cytosol, the latter of which are slightly smaller than the mitochondrial isoform. Absence of the additional bands is taken for evidence of the purity of the mitochondrial fraction. Ponceau S-stained protein was used as a loading control. D, SDO activity was determined in the mitochondria described in C ($n = 5$–10). Mean values ± SD are shown. Asterisks indicate values significantly different ($P < 0.05$) from the wild type by Student's *t* test.

($n = 4$). Thiosulfate was not produced by recombinant ETHE1.

ETHE1 Is Part of a Mitochondrial Sulfur Catabolic Pathway

To test which sulfur compounds can serve as substrates for the ETHE1-dependent pathway, we measured oxygen consumption by isolated mitochondria upon the addition of a range of potential substrates (Fig. 2C; Supplemental Table S1). In order to discriminate between ETHE1-dependent oxygen consumption and other mitochondrial reactions, we compared activities in wild-type samples with those in *ethe1-1* and *ethe1-3*. In agreement with the identified substrates for recombinant ETHE1, specific SDO activity could be observed in isolated mitochondria after the addition of GSH and elemental sulfur or GSSG and sulfide (Fig. 2C). Interestingly, the presence of 3-mercaptopyruvate also resulted in a significant rate of oxygen consumption in wild-type mitochondria, which was absent in *ethe1-1* and strongly decreased in *ethe1-3* mitochondria, indicating that this reaction is ETHE1 dependent (Fig. 2C). Sulfide or thiosulfate was not oxidized by the mitochondria, whereas L- or D-Cys addition led to a low rate of ETHE1-independent oxygen consumption (Supplemental Table S1).

The main product of mitochondrial GSSH oxidation was thiosulfate (Fig. 2D). During the standard activity test using GSH and elemental sulfur as a substrate (0.25 mg mL^{-1} mitochondrial protein, 15 min), mitochondria produced 55 ± 18 μM thiosulfate and 9 ± 10 μM sulfite while consuming 103 ± 25 μM oxygen ($n = 5$). Thus, most of the sulfite produced by the SDO reaction is immediately converted to thiosulfate in Arabidopsis mitochondria, similar to the pathway in animals (Hildebrandt and Grieshaber, 2008).

The Mitochondrial Sulfur Catabolic Pathway Is Involved in Sulfide Detoxification

To test a potential role of ETHE1 in the detoxification of excess H_2S in vivo, wild-type and *ethe1-1* plants were exposed to a sublethal concentration of H_2S (1 μL L^{-1}) for 12 d. We measured leaf contents of Cys and GSH, which are produced from sulfide during the sulfur assimilation pathway, as well as of the Cys precursor *O*-acetylserine (OAS). In addition, the inorganic products of sulfide oxidation, thiosulfate, sulfite, and sulfate, were analyzed (Fig. 3). Under control conditions, *ethe1-1* plants had significantly higher contents of Cys, GSH, and sulfate than the wild type but decreased levels of thiosulfate and OAS.

In wild-type plants, H_2S exposure resulted in a 5-fold increase of the endogenous sulfide concentration. Cys and GSH accumulated with a concomitant decrease in the precursor OAS, indicating that part of the excess sulfide was incorporated into amino acids. In addition, we found evidence for sulfide oxidation. Concentrations of thiosulfate, sulfite, and sulfate were significantly higher in H_2S-treated than in control plants. Thiosulfate increased

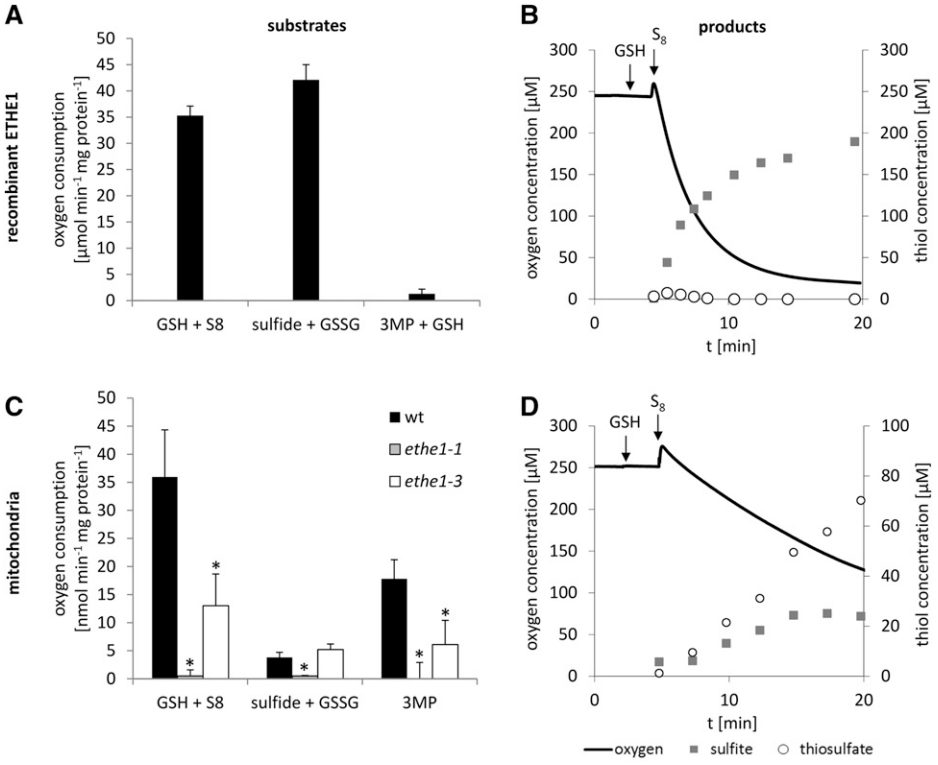

Figure 2. Substrates and products of ETHE1. A, SDO activity of recombinant ETHE1 was measured as oxygen consumption using a Clarke-type oxygen electrode. One millimolar GSH plus 15 μL mL^{-1} saturated acetonic solution of elemental sulfur (S8), 3 mM sulfide plus 0.5 mM GSSG preincubated at 30°C for 10 min, and 5 mM 3-mercaptopyruvate (3MP) plus 1 mM GSH were used as substrates (n = 3). B, Original traces of an SDO activity test for recombinant ETHE1 (1.5 μg protein mL^{-1}). One millimolar GSH and 15 μL mL^{-1} saturated acetonic solution of elemental sulfur were added (indicated by arrows) to produce the substrate GSSH nonenzymatically. The oxygen concentration was measured using an oxygen electrode, and concentrations of sulfite and thiosulfate were quantified by HPLC. C, SDO activity of mitochondria isolated from wild-type (wt), *ethe1-1*, and *ethe1-3* cell suspension cultures was measured as oxygen consumption. One millimolar GSH plus 15 μL mL^{-1} elemental sulfur, 1 mM sulfide plus 1 mM GSSG, and 5 mM 3-mercaptopyruvate were used as substrates (n = 3). D, Original traces of an SDO activity test for wild-type Arabidopsis mitochondria (0.25 mg protein mL^{-1}). Conditions were the same as in B. Asterisks indicate values significantly different ($P < 0.05$) from the wild type by Student's t test.

most drastically (1,588-fold), from 3.8 ± 0.3 to 6,002 ± 117 pmol mg^{-1} fresh weight, so that after the H_2S exposure it became one of the most abundant sulfur compounds present in the leaves. The accumulation of thiosulfate and sulfite upon sulfide exposure was significantly less pronounced in *ethe1-1* plants than in the wild type, and the sulfate concentration even decreased, indicating a role of the ETHE1-dependent mitochondrial sulfur catabolic pathway in sulfide oxidation. Thus, the results of in planta analysis of *ethe1* mutants are in full agreement with the biochemical characterization of ETHE1 recombinant protein and isolated mitochondria and demonstrate the relevance of ETHE1 for the detoxification of sulfide derived from Cys degradation.

Low Levels of ETHE1 Are Sufficient for the Survival of Arabidopsis Plants, But Development Is Delayed

While complete knockout of the *ETHE1* gene is embryo lethal (Holdorf et al., 2012), seeds of the strong knockdown mutant *ethe1-1* were viable. However, we observed a severe delay in embryo development (Fig. 4, A and B). Five days after pollination, most of the *ethe1-1* embryos were still at the globular stage and reached the heart stage only 7 d after pollination, whereas wild-type embryos were already at the heart stage and the bent cotyledon or mature stage. The development of *ethe1-1* plants grown under long-day conditions was also delayed (Fig. 4, C and D). Growth rates of *ethe1-1* rosettes expressed as diameter and number of leaves were about 60% of the wild-type rates (Supplemental Fig. S2). There were no apparent differences regarding embryo development or growth phenotype between wild-type plants and the weaker knockdown lines *ethe1-2* and *ethe1-3*.

ETHE1 Is Involved in Mitochondrial Amino Acid Catabolism

We used the information available from a proteomic approach in combination with coexpression analysis to elucidate in which physiological context ETHE1 activity

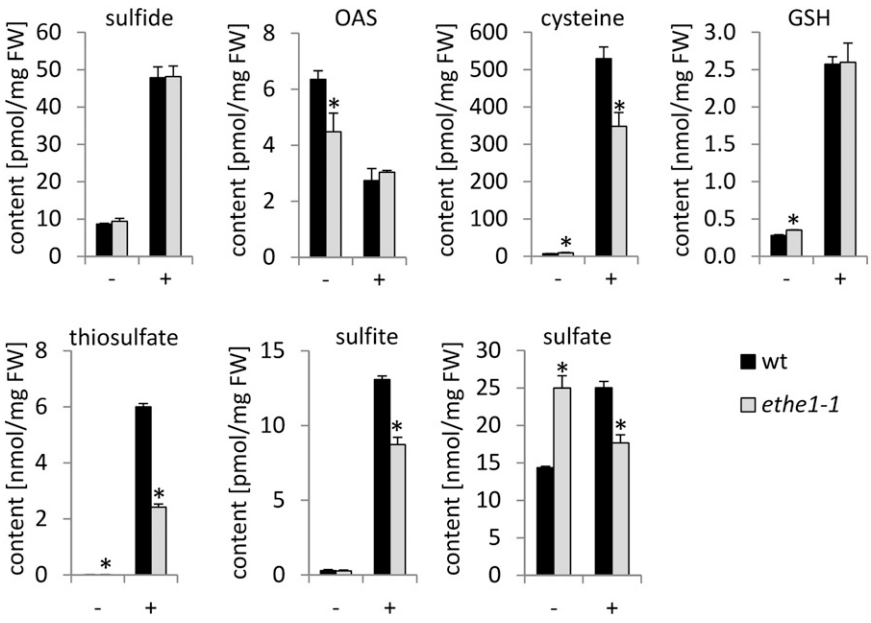

Figure 3. Products of sulfide metabolism in wild-type (wt) and *ethe1-1* plants. Sulfur-containing metabolites were extracted from aerial parts of wild-type and *ethe1-1* plants grown under short-day conditions for 4 weeks followed by exposure to 0 (−) or 1 (+) ppm H_2S for 12 d and quantified using HPLC ($n = 3$). FW, Fresh weight. Asterisks indicate values significantly different ($P < 0.05$) from the wild type by Student's *t* test.

is most relevant for plant metabolism. Mitochondria isolated from wild-type and *ethe1-1* cell suspension cultures were analyzed by isoelectric focusing (IEF)/SDS-PAGE, and 73 proteins were identified in 45 spots with a significantly changed volume (Table I; Supplemental Fig. S3; Supplemental Table S2).

Our results confirm the predicted role of ETHE1 in plant sulfur metabolism. Several enzymes involved in Cys synthesis (Ser acetyltransferase and Ser hydroxymethyltransferase) or degradation (β-cyanoalanine synthase, Asp aminotransferase, NSF1, nitrogen fixation factor U-like domain containing protein4 [NFU4], and NFU5) were affected in *ethe1-1* mitochondria. Interestingly, we also found indications for differences in energy metabolism between *ethe1-1* and the wild type. Tricarboxylic acid cycle dehydrogenases (malate dehydrogenase, succinate dehydrogenase, subunits of pyruvate and 2-oxoglutarate dehydrogenase complexes) as well as enzymes involved in the oxidation of amino acids as alternative substrates of the mitochondrial respiratory chain (e.g. electron-transfer flavoprotein [ETF], electron-transfer flavoprotein:ubiquinone oxidoreductase [ETFQO], branched-chain α-keto acid dehydrogenase, fumarylacetoacetate hydrolase, methylcrotonoyl-CoA carboxylase, and Glu dehydrogenase) were detected in spots with a changed volume (Table I). This data set provides valuable information about which mitochondrial pathways in general are affected by the *ETHE1* knockdown. However, care must be taken not to overinterpret the results. Regulation patterns of individual enzymes cannot be concluded, since spot volume is not always equivalent to the total abundance of one specific protein.

The potential role of ETHE1 in amino acid catabolism is further supported by coexpression analysis using Genevestigator (www.genevestigator.com). *ETHE1* expression was up-regulated in experiments that stimulate nutrient remobilization, such as prolonged darkness, drought, abscisic acid treatment, and germination. Enzymes involved in protein degradation and amino acid catabolism as well as peroxisomal fatty acid β-oxidation were most clearly coexpressed with ETHE1 under these conditions (Supplemental Table S3). In particular, several enzymes of the BCAA and Lys catabolic pathway (ETF, isovaleryl-CoA dehydrogenase, 3-hydroxyisobutyrate dehydrogenase, branched-chain α-keto acid dehydrogenase subunits, and aminoadipate-semialdehyde dehydrogenase) showed an expression pattern similar to ETHE1. Thus, equivalent to the situation in animals, Arabidopsis ETHE1 is probably involved in sulfur metabolism as well as mitochondrial amino acid oxidation.

ETHE1 Has an Essential Function in the Use of Amino Acids as Respiratory Substrates during Carbohydrate Starvation

The identification of a potential role of ETHE1 in amino acid catabolism prompted us to further investigate the phenotype and amino acid profiles of *ethe1-1* compared with wild-type plants under conditions with increased protein degradation. These include senescence, decreased light availability (short-day conditions), and severe carbohydrate starvation caused by extended darkness (Fig. 5). The *ethe1-1* mutant was sensitive to changes in the photosynthetically active period, showing premature senescence under light-limiting conditions. When the plants were grown under long-day conditions (16 h of light/8 h of dark), rosette leaves of *ethe1-1* plants appeared pale green compared with the wild type, but otherwise senescence proceeded in a similar fashion (Fig. 5A; Supplemental Fig. S4A). Under short-day conditions (8 h of light/16 h of dark), the oldest

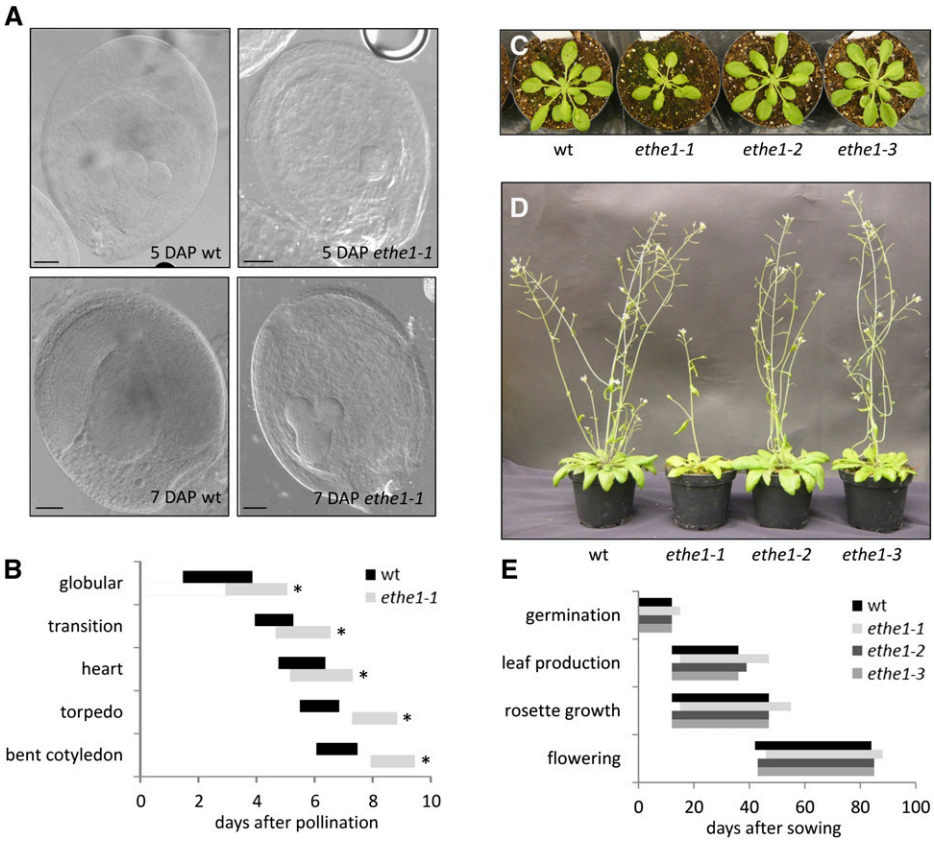

Figure 4. Phenotype of ETHE1 knockdown mutants grown under long-day conditions. A, Representative images of embryos in seeds of wild-type (wt) plants and *ethe1-1* mutants at 5 and 7 d after pollination (DAP). Bars = 50 μm. B, Progression of embryo development in the wild type and *ethe1-1*. A total of 224 siliques between 1 and 12 DAP from four different plants were analyzed for the wild type and mutant, and bars indicate the mean age ± SD of embryos in the different developmental stages. Asterisks indicate values significantly different ($P < 0.05$) from the wild type by the Mann-Whitney rank sum test. C, Rosettes of wild-type plants and the *ethe1* mutant lines 40 d after sowing. D, Mature wild-type and mutant plants 56 d after sowing. E, Principal growth stages according to Boyes et al. (2001). Bars represent mean values for the duration of the stages for wild-type plants and *ethe1* mutant lines ($n = 10$). [See online article for color version of this figure.]

leaves of *ethe1-1* plants became chlorotic after 7 weeks of growth starting at the edges (Fig. 5B, arrows). In the further course of development, leaves of the mutant plants turned upward and showed progressive signs of senescence, while wild-type rosettes continued to grow and stayed dark green (Supplemental Fig. S4B). This phenotype became more pronounced when plants were grown in extended darkness (Fig. 5C).

To test whether an increase in reactive oxygen species (ROS) production contributes to premature leaf senescence in *ethe1-1* plants, we analyzed hydrogen peroxide (H_2O_2) and superoxide levels in young leaves of plants grown under short-day conditions by 3,3′-diaminobenzidine (DAB) and nitroblue tetrazolium (NBT) staining, respectively (Supplemental Fig. S5). H_2O_2 production was not significantly different in *ethe1-1* compared with the wild type and was clearly restricted to necrotic leaf areas (Supplemental Fig. S5A). In contrast, NBT-stained portions of *ethe1-1* leaves (37% ± 26%) were significantly larger than in the wild type (19% ± 9%) and not correlated to visible signs of senescence. Interestingly, formazan production is not specific for superoxide, but NBT is also rapidly reduced by GSSH (Supplemental Fig. S5D). Thus, our results indicate a general increase in ROS or reactive sulfur species in *ethe1-1* plants.

In agreement with the postulated function of ETHE1 in protein catabolism, we found an accumulation of all detectable amino acids in seeds from *ethe1-1* plants compared with the wild type during early embryo development (4–5 d after pollination), resulting in a 1.8-fold increase of total free amino acid content (Supplemental Table S4). The amino acid composition was not changed in senescent rosette leaves of *ethe1-1* plants grown under long-day conditions (Fig. 5D; Supplemental Table S5). However, under short-day conditions, concentrations of the compounds related to sulfur metabolism (Cys, glutathione, and Ser) as well as the BCAA Val, Leu, and Ile were significantly higher in the mutant than in the wild type (Fig. 5D; Supplemental Table S5). The effect on amino acid content became more pronounced when plants were subjected to complete darkness for 7 d. The largest differences between *ethe1-1* and the wild type again occurred in sulfur-containing amino acids (2- to 5-fold) and BCAA (3- to 6-fold). In addition, extended darkness generally led to a drastic (50- to 60-fold) increase in the nitrogen-rich amino acids Arg and Asn, and concentrations were slightly higher in *ethe1-1* than in wild-type leaves (Supplemental Table S5). As a consequence, the total concentration of free amino acids increased 4-fold in wild-type leaves and 5-fold in *ethe1-1*

Table I. *Proteins with potentially changed abundance in ethe1-1 mitochondria*

Mitochondrial proteins from wild-type and *ethe1-1* cell culture were separated by IEF/SDS-PAGE (Supplemental Fig. S3). Gels from three biological replicates were analyzed by Delta2D (Decodon), and the proteins in spots with at least 1.5-fold changes in volume were identified by nano-liquid chromatography-tandem mass spectrometry. For additional information, see Supplemental Table S2.

Spot	Accession No.	Name	Ratio[a]	Spot	Accession No.	Name	Ratio[a]
1	AT3G55410	E1 2-oxoglutarate dehydrogenase	4.23	25	AT1G51390	NifU5	0.66
2	AT3G61440	β-Cyanoalanine synthase	3.98	26	AT5G07440	Glu dehydrogenase	0.63
3	AT2G05710	Aconitase	3.06	27	AT1G65290	Acyl carrier protein	0.63
4	AT3G10920	Superoxide dismutase	2.92	28	AT1G06530	Tropomyosin-related protein	0.63
5	AT3G55410	E1 2-oxoglutarate dehydrogenase	2.90	28	AT4G26780	Chaperone	0.63
6	AT2G29530	Tim10 (for 10-kD subunit of the preprotein translocase of the inner mitochondrial membrane)	2.54	29	AT2G30970	Asp aminotransferase	0.62
				30	AT3G20970	NifU4	0.61
				31	AT2G28000	Chaperonin 60α	0.61
7	AT2G45060	Hypothetical protein	2.41	31	AT3G02650	TPR-like protein	0.61
7	AT1G53240	Malate dehydrogenase	2.41	32	AT4G35090	Catalase	0.61
7	AT2G30920	Hexaprenyl methyltransferase	2.41	33	AT5G62690	Tubulin	0.60
7	AT3G18580	Single-stranded DNA-binding protein	2.41	34	AT5G66760	Succinate dehydrogenase	0.60
7	AT5G13450	ATP synthase subunit O	2.41	35	AT2G07698	ATP synthase subunit α	0.58
7	AT4G26910	E2 2-oxoglutarate dehydrogenase	2.41	35	AT1G48030	E3 dihydrolipoyl dehydrogenase	0.58
7	AT5G23140	Caseinolytic protease	2.41	36	AT2G43400	ETFQO	0.58
8	AT5G18170	Glu dehydrogenase	2.41	37	AT3G58610	Ketol-acid reductoisomerase	0.55
9	AT5G26780	Ser hydroxymethyltransferase	2.38	38	AT2G33210	Chaperonin CPN60	0.53
9	AT5G62530	δ-Pyrroline-5-carboxylate dehydrogenase	2.38	38	AT5G04740	ACT domain-containing protein	0.53
10	AT2G42210	Tim17 domain-containing protein	2.36	39	AT2G43090	3-Isopropylmalate dehydratase	0.50
11	AT4G34030	Methylcrotonyl-CoA carboxylase	2.17	40	AT3G23990	Chaperonin CPN60	0.49
12	AT3G06850	E2 branched-chain α-keto acid dehydrogenase	2.04	41	AT3G43810	Calmodulin	0.37
				42	AT1G22300	General regulatory factor10 (GRF10; 14-3-3-like)	0.37
13	AT3G13930	E2 pyruvate dehydrogenase	2.01				
14	AT5G65750	E1 2-oxoglutarate dehydrogenase	1.96	42	AT5G38480	GRF3 (14-3-3-like)	0.37
14	AT2G22780	Malate dehydrogenase	1.96	42	AT4G22240	Lipid-associated protein	0.37
15	AT3G02780	Isopentenyl-diphosphate δ-isomerase	1.89	43	AT1G54580	Acyl carrier protein	0.29
15	AT2G21870	ATP synthase subunit	1.89	44	AT4G24280	Heat shock 70-kD protein (HSP70-1)	0.28
16	AT4G05400	Copper ion-binding protein	1.84				
17	AT4G34700	Complex I β-subcomplex 9	1.83	45	AT1G66410	Calmodulin	0.24
18	AT5G08530	Complex I flavoprotein1	1.73				
18	AT2G07698	ATP synthase subunit α	1.73				
19	AT3G13110	Ser acetyltransferase	1.66				
19	AT3G26760	Rossmann fold-containing protein	1.66				
19	AT5G20080	NADH-cytochrome b_5 reductase	1.66				
19	AT5G63400	Adenylate kinase	1.66				
20	AT5G66510	γ-Carbonic anhydrase	1.64				
20	AT5G43430	Electron transfer flavoprotein	1.64				
20	AT5G15090	VDAC3 (for Mitochondrial outer membrane protein porin3)	1.64				
21	AT2G05710	Aconitase	1.62				
21	AT5G08670	ATP synthase subunit β	1.62				
21	AT3G17240	E3 dihydrolipoyl dehydrogenase	1.62				
21	AT1G63940	Monodehydroascorbate reductase	1.62				
22	AT3G18580	Single-stranded DNA-binding protein	1.62				
22	AT2G31140	Peptidase	1.62				
22	AT4G15640	Unknown protein	1.62				
22	AT4G15940	Fumarylacetoacetate hydrolase	1.62				
22	AT5G13450	ATP synthase subunit O	1.62				
23	AT5G65720	Cys desulfurase (NifS)	1.60				
24	AT5G26780	Ser hydroxymethyltransferase	1.53				

[a]Ratio of mean spot volume on *ethe1-1* gels to mean spot volume on wild-type gels.

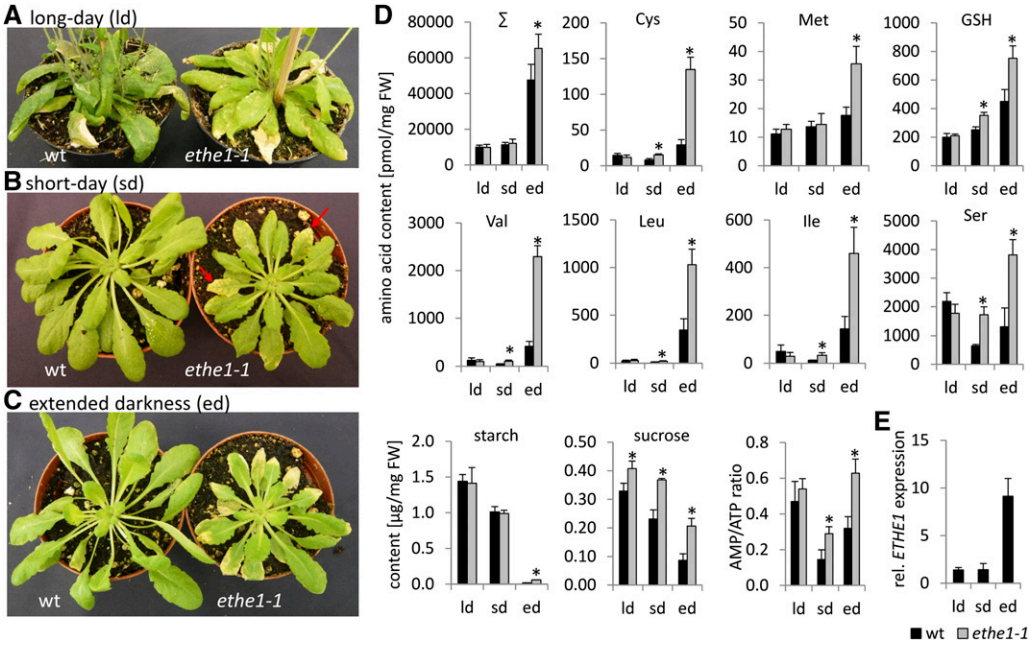

Figure 5. Phenotypes and metabolite profiles of wild-type and *ethe1-1* plants under conditions stimulating protein degradation. A to C, Rosettes of wild-type (wt) and *ethe1-1* plants after 13 weeks of growth under long-day conditions (ld; 16 h of light/8 h of dark; A), after 7 weeks of growth under short-day conditions (sd; 8 h of light/16 h of dark; B), and after 7 d of extended darkness (ed) following 7 weeks of growth under short-day conditions (C). D, Amino acids and GSH, carbohydrates, and adenylates were extracted from rosette leaves of wild-type and *ethe1-1* plants grown under the conditions shown in A to C and quantified using HPLC ($n = 5$). Σ, Sum of all detectable free amino acids, and starch content is shown as Glc equivalents. Asterisks indicate values significantly different ($P < 0.05$) from the wild type by Student's *t* test. For complete amino acid, carbohydrate, and adenylate profiles, see Supplemental Table S5. FW, Fresh weight. E, Relative *ETHE1* transcript levels in rosette leaves of wild-type plants during the conditions shown in A to C were determined by quantitative RT-PCR ($n = 5$). Transcript levels of *ETHE1* were normalized to cytosolic *GAPDH* (AT1G13440).

leaves compared with short-day conditions, resulting in a significantly higher total amino acid concentration in mutant than in wild-type plants (65.3 ± 7.9 versus 47.6 ± 8.8 nmol mg^{-1} fresh weight). Surprisingly, there were no significant differences in the contents of sulfide, thiosulfate, or sulfite between wild-type and mutant plants upon extended dark treatment (Supplemental Table S6).

To better characterize the effect of *ETHE1* knockdown on energy metabolism, we analyzed leaf carbohydrate and adenylate levels (Fig. 5D; Supplemental Table S5). As expected, starch was almost completely depleted after 7 d of darkness in wild-type and mutant plants, and concentrations of Suc as well as several monosaccharides also decreased significantly. Differences in metabolite contents between *ethe1-1* and the wild type were again most pronounced in the dark-treated plants. Levels of starch, Suc, Glc, and Fru as well as total adenylate concentrations (ATP, ADP, and AMP) were elevated in *ethe1-1* compared with wild-type leaves. However, the AMP-ATP ratio, an indicator of low cellular energy status, was also significantly higher in *ethe1-1* than in wild-type plants under short-day conditions and extended darkness (Fig. 5D).

Together with the strong phenotypic effects, the changes in the metabolite profile of mutant plants point toward a pivotal role of ETHE1 during dark-induced carbohydrate starvation. In agreement with this, the transcript amount of *ETHE1* was 6.5-fold higher in rosette leaves of wild-type plants subjected to extended darkness compared with leaves of plants grown under long- or short-day conditions (Fig. 5E).

DISCUSSION

Plant ETHE1 has recently been identified as an SDO localized in the mitochondria with an essential but as yet undefined function in early embryo development (Holdorf et al., 2012). Here, we describe the physiological role of ETHE1 in the catabolism of sulfur-containing amino acids and BCAA based on the analysis of three Arabidopsis knockdown mutants. T-DNA insertion into the 5′ untranslated region in *ethe1-1* resulted in a strong decrease in enzyme activity to about 1% of wild-type levels, which was sufficient for plant viability but led to pronounced growth defects throughout the life cycle. A decrease in SDO activity by about 50% in *ethe1-2* and *ethe1-3* was tolerated by the plants without any obvious phenotypic effects.

The Biochemical Function of ETHE1: Sulfur Oxidation during Cys Catabolism

Increased concentrations of Cys, Met, and GSH in *ethe1* knockdown plants indicate a function of ETHE1

in sulfur amino acid metabolism. We performed biochemical studies on plants, isolated mitochondria, and recombinant ETHE1 enzyme to investigate details of this function. Our results identified a new mitochondrial pathway catalyzing the detoxification of sulfide or reduced sulfur species derived from Cys catabolism by oxidation to thiosulfate (Fig. 6).

In plants, free sulfide is normally rapidly incorporated into Cys by the different OAS (thiol) lyase isoforms (Hell and Wirtz, 2011). However, an alternative route is required for the degradation of sulfur-containing amino acids. Exposure of Arabidopsis plants to environmental H_2S demonstrated that thiosulfate is a major product of sulfide detoxification and ETHE1 is involved in its production. Since thiosulfate was also the main product of persulfide oxidation in Arabidopsis mitochondria, we postulate that, analogous to the reaction sequence in animals, a sulfurtransferase converts the sulfite produced by ETHE1 to thiosulfate. According to our results, Cys catabolism in plants most likely involves transamination to 3-mercaptopyruvate, which is then oxidized by the ETHE1 pathway. The thiol group is probably transferred from 3-mercaptopyruvate to GSH, since ETHE1 is highly specific for GSSH as a substrate, and this reaction could be catalyzed by mercaptopyruvate sulfurtransferase. A functional connection between ETHE1 and the main mitochondrial sulfurtransferase in Arabidopsis, STR1 (AT1G79230), is supported by the phenotype of knockout mutants. STR1 deficiency leads to a delay in early embryo development similar to ETHE1 deficiency (Mao et al., 2011).

Alternatively, Cys degradation could proceed via desulfhydration to sulfide, pyruvate, and ammonia by DES1 (AT5G28030), which has been shown to regulate Cys homeostasis during senescence and environmental stress (Alvarez et al., 2010). However, we found that Arabidopsis mitochondria were not able to oxidize sulfide, and there is no homolog of the enzyme catalyzing sulfide oxidation in animals (sulfide to quinone oxidoreductase) encoded by plant genomes. Thus, in Arabidopsis, the first oxidation step of sulfide to persulfide is either catalyzed by a currently unknown cytosolic enzyme or depends on nonenzymatic GSSH production in the presence of GSSG.

The Physiological Context of ETHE1: Amino Acid Catabolism for ATP Production

Several lines of evidence indicate that, in addition to its role in Cys catabolism, ETHE1 is probably involved in energy metabolism and the use of amino acids as alternative respiratory substrates during carbohydrate starvation. Under conditions of low sugar availability such as extended darkness, drought, or extreme temperatures, fatty acids are oxidized by peroxisomal β-oxidation, and in addition, cellular proteins and entire organelles are degraded by autophagy to produce amino acids as an energy source (Araújo et al., 2011). Especially BCAA, aromatic amino acids, and Lys have a key function as substrates for ATP production (Izumi et al., 2013). The pathways oxidizing these amino acids are localized in the mitochondria and transfer electrons into the respiratory chain via the ETF/ETFQO complex (Taylor et al., 2004; Araújo et al., 2010).

Coexpression analysis as well as mitochondrial proteomics clearly placed ETHE1 in the functional context of carbohydrate starvation, and *ETHE1* expression was indeed induced by extended darkness. In agreement with these results, phenotypic defects of *ETHE1* knockdown plants were more pronounced under light-limiting conditions. Plants developed starvation-induced chlorosis, which is similar to the phenotype produced by defects in autophagy or the ETF/ETFQO system and associated dehydrogenases (Ishizaki et al., 2005, 2006; Araújo et al., 2010; Izumi et al., 2013). The amino acid profile of *ethe1* mutants, which in addition to an accumulation of sulfur amino acids revealed an increase in BCAA characteristic for alternative respiration defects, suggests a specific role of ETHE1 in this pathway. Although premature chlorosis

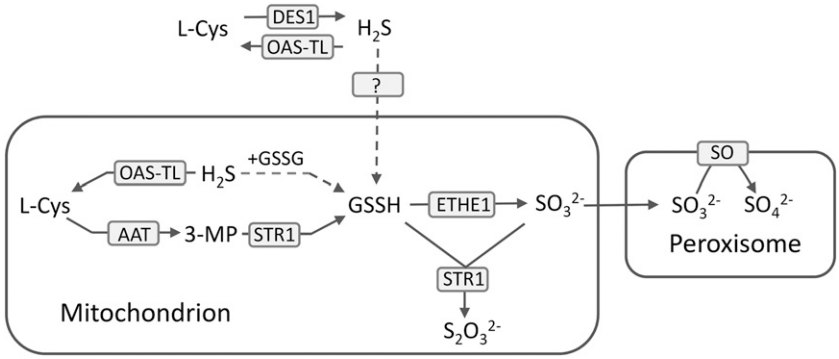

Figure 6. Model of Cys catabolic pathways in Arabidopsis. In the cytosol, Cys is desulfurated by DES1, producing H_2S. Sulfide is oxidized to GSSH either nonenzymatically in the presence of GSSG or catalyzed by a currently unknown cytosolic enzyme. In the mitochondrial matrix, Cys is converted to 3-mercaptopyruvate (3-MP) by an aminotransferase (AAT) before a sulfurtransferase (STR1) transfers the persulfide group to an acceptor such as GSH, producing GSSH. ETHE1 oxidizes GSSH to sulfite (SO_3^{2-}), which is either converted to thiosulfate ($S_2O_3^{2-}$) via the addition of a persulfide group by STR1 or transported to the peroxisomes for oxidation to sulfate (SO_4^{2-}) by sulfite oxidase (SO; Lang et al., 2007; Brychkova et al., 2013). OAS-TL, OAS (thiol) lyase.

and leaf senescence clearly indicate an energy shortage, depletion of starch, sugar, and ATP was not accelerated in *ethe1-1* plants. Similar findings from previous studies demonstrate that metabolic adaptations to energy deprivation in plants can be complex. Low concentrations of malate and fumarate lead to accelerated dark-induced senescence in a malic enzyme-overexpressing Arabidopsis line, while sugar levels are high (Fahnenstich et al., 2007). Down-regulation of different respiratory chain complexes restricts growth despite unchanged or even increased steady-state ATP levels (Szal et al., 2008; Robison et al., 2009; Geisler et al., 2012). The high AMP-ATP ratio in *ethe1-1* plants could induce a broad transcriptional response to stress and energy deprivation mediated by AMP-activated protein kinases such as KIN10 (AT3G01090), which is coexpressed with *ETHE1* (Baena-González et al., 2007).

The amino acid profile of young *ethe1-1* seeds is again strikingly similar to defects in isovaleryl-CoA dehydrogenase, which is involved in the degradation of BCAA (Gu et al., 2010). In contrast to knockout mutants for Lys-ketoglutarate reductase/saccharopine dehydrogenase or Thr aldolase, which very specifically accumulate Lys or Thr in the seeds (Zhu et al., 2001; Jander et al., 2004), isovaleryl-CoA dehydrogenase deficiency leads to a general increase in free amino acids similar to ETHE1 deficiency (Gu et al., 2010). Thus, BCAA catabolism plays an important role in regulating amino acid levels in seeds, and inhibition of this pathway in *ethe1* mutants might interfere with the nutrient supply to the developing embryo. However, since defects in embryogenesis are not described for any of the mutants related to autophagy or the use of amino acids as respiratory substrates (Ishizaki et al., 2005, 2006; Araújo et al., 2010; Gu et al., 2010; Izumi et al., 2013), the severe consequences of ETHE1 deficiency indicate additional problems. Lack of the mitochondrial sulfurtransferase STR1, which we suggest is involved in the same pathway as ETHE1, also impairs embryogenesis (Mao et al., 2011). Thus, seed abortion seems to be an immediate consequence of the block in sulfur catabolism, possibly caused by an increase in toxic intermediates such as sulfide or reactive persulfide compounds. This hypothesis will have to be tested (e.g. with *ethe1/str1* double mutants). In humans suffering from ethylmalonic encephalopathy, C4 and C5 acylcarnitines and acylglycines accumulate in the bloodstream, indicating a block in fatty acid and BCAA oxidation at the level of acyl-CoA. Indeed, H_2S has been shown to inhibit short-chain acyl-CoA dehydrogenase in vitro, so that the increase in tissue sulfide concentrations caused by ETHE1 deficiency is thought to be responsible for the metabolite profile of the patients (Tiranti et al., 2009). However, sulfide concentrations were normal in *ethe1-1* leaves. Another possible explanation is the inhibition of acyl-CoA dehydrogenases by CoA persulfides (Shaw and Engel, 1987), which are likely to accumulate when high concentrations of reduced sulfur are present. The increased intensity of NBT staining in *ethe1-1* leaves without changes in H_2O_2 production indicate that the block in persulfide oxidation probably leads to an accumulation of reactive sulfur species. Indirect pleiotropic effects such as a decrease in respiratory chain activity and inactivation of additional enzymes by increased ROS levels could also play a role. Proteome studies in ETHE1-deficient mice have further indicated a possible regulatory effect via posttranslational protein modifications (Hildebrandt et al., 2013). Thus, our results clearly demonstrate the central function of Arabidopsis ETHE1 in metabolic adaptation to prolonged darkness. Additional experiments will be necessary to clarify mechanistic aspects and distinguish between a direct role of ETHE1 in BCAA catabolism versus general effects on energy homeostasis.

CONCLUSION

In summary, this study identified the physiological role of ETHE1, which is in amino acid catabolism. The SDO detoxifies reactive intermediates in the degradation of sulfur-containing amino acids and strongly affects the oxidation of BCAA as alternative respiratory substrates in situations of carbohydrate starvation. Therefore, ETHE1 is expected to be relevant for plant productivity during seed production as well as for stress tolerance against drought or shading.

MATERIALS AND METHODS

Plant Material and Growth Conditions

All Arabidopsis (*Arabidopsis thaliana*) plants used for this study were of the Columbia ecotype. Plants were grown in climate chambers under long-day conditions (16 h of light/8 h of dark) or short-day conditions (8 h of light/16 h of dark) at 22°C, 85 μmol s^{-1} m^{-2} light, and 65% humidity. The T-DNA insertion lines SALK_021573 (*ethe1-1*), SALK_091956 (*ethe1-2*), and SALK_127065 (*ethe1-3*) for the gene *AT1G53580* were obtained from the Nottingham Arabidopsis Stock Centre (University of Nottingham).

Plants for fumigation experiments were germinated and grown on soil under short-day conditions. Three-week-old plants were transferred into fumigation cabinets to allow acclimatization for 1 week. Subsequently, plants were exposed to sulfide (1 ppm H_2S) for 12 d according to Buchner et al. (2004).

For dark treatment, plants were grown under short-day conditions for 7 weeks and then transferred to darkness for 7 d. Before and after the dark treatment, complete rosettes of five wild-type and mutant plants were harvested and used for metabolite analysis.

Isolation of T-DNA Insertion Mutants and Genotype Characterization

Homozygous mutant lines were identified by genomic PCR using gene-specific primers (5′-TGGAATTGGGTTATATGGTGG-3′ and 5′-CGGATCAATCAACTGCTCATC-3′ for *ethe1-1*, 5′-TGGAATTGGGTTATATGGTGG-3′ and 5′-CCCATGTCGAAAAATTCAATC-3′ for *ethe1-2*, and 5′-TCATGGATTCGTGGTATACCG-3′ and 5′-CGGATCAATCAACTGCTCATC-3′ for *ethe1-3*) and the T-DNA left border primer LBb1.3 (5′-ATTTTGCCGATTTCGGAAC-3′). PCR products were sequenced by Seqlab to determine the exact T-DNA insertion sites. ETHE1 expression was analyzed by quantitative reverse transcription (RT)-PCR as described by Niessen et al. (2012). Primer combinations were 5′-AAGGTTTCGAGGTAAGTACAGTTGG-3′ and 5′-CTTGAGAAGGCACATCTTGTAACC-3′ for ETHE1 and 5′-GGAATCTGAAGGCAAAATGAAGG-3′ and 5′-TGTTGTCACCAACAAAGTCGG-3′ for glyceraldehyde-3-phosphate dehydrogenase (GAPDH; AT1G13440).

Expression and Purification of ETHE1

The coding sequence of AT1G53580 was cloned into the pET28a(+) expression vector in frame with a C-terminal 6× His tag using the primers

5′-CATCCATGGGTAAGCTTCTCTTTCGTCAACTC-3′ and 5′-GCGCCTCG-AGGTTGGCTTGAGAAGGCACATC-3′. The first 50 codons containing the mitochondrial targeting sequence were removed and replaced by a Met and a Gly codon, generating the N-terminal amino acid sequence MGKLLFRQ. After verification of the nucleotide sequence, the plasmid was transformed into *Escherichia coli* strain BL21(DE3)pLYS. Expression was induced by the addition of isopropyl-β-D-thiogalactopyranoside to a final concentration of 0.2 mM, followed by incubation at 18°C overnight with shaking. Cell-free lysate in 50 mM $NaPO_4$, 300 mM NaCl, and 10 mM imidazole, pH 8.0, was applied to a 1-mL HisTrap HP column (GE Healthcare) and eluted with a 10 to 250 mM imidazole gradient. ETHE1 purified as a single peak (Supplemental Fig. S1A). We obtained a high yield of soluble protein with an electrophoretic mobility of 28 kD, which is in agreement with the calculated molecular mass of 28,008 D for the monomer (Supplemental Fig. S1A). The purified protein contained 0.5 atoms of Fe^{2+} per monomer, as reported previously (McCoy et al., 2006; Tiranti et al., 2009). Preincubation of the enzyme with 1 M equivalent of Fe and addition of 2.5 mM ascorbate did not increase SDO activity.

The plasmid containing human ETHE1 was generously provided by Valeria Tiranti and Massimo Zeviani (The Foundation of the Carlo Besta Neurological Institute) and expressed in the same way as Arabidopsis ETHE1.

SDO Activity Test

SDO activity was measured at 25°C in a Clarke-type oxygen electrode (Oroboros Oxygraph and Hansatech DW1 Oxygraph) following the procedure described by Hildebrandt and Grieshaber (2008). The reaction contained 1 to 2 $\mu g\ mL^{-1}$ of purified enzyme or 150 to 300 $\mu g\ mL^{-1}$ of mitochondrial protein in 0.1 M KPO_4, pH 7.4. For the standard activity test, 1 mM GSH (final concentration) was added, followed by 15 $\mu L\ mL^{-1}$ of a saturated elemental sulfur solution in acetone. Acetone did not inhibit enzyme activity. Rates were measured during the linear phase of oxygen depletion, which occurred in the first 2 to 3 min.

Phenotype Analysis

For general phenotype analysis, a modified version of the procedure described by Boyes et al. (2001) was used. Plants were grown under long-day conditions, and growth parameters were measured three times per week.

Embryo morphology was analyzed with a microscope equipped with Nomarski optics. Siliques were cleared in Hoyer's solution (15 mL of distilled water, 3.75 g of gum arabic, 2.5 mL of glycerine, and 50 g of chloral hydrate) overnight before seeds were dissected.

Histochemical Detection of H_2O_2 and Superoxide

Histochemical detection of H_2O_2 was performed as described by Thordal-Christensen et al. (1997) with slight modifications. Rosette leaves were incubated in DAB staining solution (1 mg mL^{-1} DAB, 0.05% [v/v] Tween 20, and 10 mM Na_2HPO_4) for 7 h. Superoxide was detected by formazan staining for 5 h in 0.1 mg mL^{-1} NBT and 25 mM HEPES, pH 7.6. After DAB or NBT staining, chlorophyll was removed by boiling the leaves in bleaching solution (ethanol:acetic acid:glycerol, 3:1:1) for 15 min. H_2O_2 produced a reddish brown precipitate, and superoxide was visualized as a purple formazan deposit within leaf tissues. Stained leaf areas were quantified using ImageJ software (http://imagej.nih.gov/ij/).

Metabolite Analysis

Products of the SDO reaction were analyzed by HPLC (Hildebrandt and Grieshaber, 2008). Hydrophilic metabolites were extracted from 50 mg of leaf material as described by Wirtz and Hell (2003). Derivatization, separation, and quantification of thiols, OAS, amino acids, and sulfate were performed as described by Heeg et al. (2008). Sulfite, sulfide, and thiosulfate were determined according to Birke et al. (2012).

Soluble sugars were extracted from powdered plant material (50 mg) by incubation with 0.5 mL of 80% (v/v) ethanol for 45 min at 80°C. Cell debris and insoluble starch were removed by centrifugation for 10 min at 25,000*g* and 4°C. Soluble sugars of the resulting supernatant were separated with a gradient of 15 to 300 mM NaOH on a CarboPac PA1 column connected to an ICS-3000 system (Dionex) and quantified by high-performance anion-exchange chromatography-pulsed amperometric detection. Data acquisition and quantification were performed with Chromeleon 6.7 (Dionex). For the quantification of starch, the sediment of soluble sugar extraction was washed twice with 80% ethanol and resuspended in 0.2 mL of 0.2 M KOH. Starch was partly hydrolyzed by incubation at 95°C for 1 h and subsequently digested in 25 mM sodium acetate, pH 5.2, with 0.1 unit of amyloglucosidase for 16 h at 37°C. The resulting Glc was quantified by high-performance anion-exchange chromatography-pulsed amperometric detection as described above.

Adenylates were quantified as described by Bürstenbinder et al. (2010).

Cell Suspension Cultures and Isolation of Mitochondria

Arabidopsis cell suspension cultures were established and maintained as described by May and Leaver (1993) and Sunderhaus et al. (2006). Briefly, Arabidopsis seeds were surface sterilized, plated on solid Murashige and Skoog medium (0.44% [w/v] Murashige and Skoog medium [Duchefa], 2% [w/v] Suc, and 1% [w/v] agar, pH 5.7), and grown for 10 d under long-day conditions. Callus formation was induced by incubating stem explants on solid callus induction medium (0.316% [w/v] Gamborg's B5 medium [Duchefa], 3% [w/v] Suc, 1% [w/v] agar, 0.5 mg L^{-1} 2,4-dichlorphenoxyacetic acid, and 0.05 mg L^{-1} kinetin, pH 5.7) at 25°C in the dark. Suspension cultures were grown in 500-mL flasks containing 100 mL of liquid B5 medium (callus induction medium without agar) at 25°C and 90 rpm in the dark. Cells were transferred into fresh medium every 7 d. There were no significant differences between growth rates of wild-type cells and the *ethe1* mutants. Mitochondria were prepared following to the procedure outlined by Werhahn et al. (2001). The high purity of mitochondria prepared according to this method has been demonstrated by proteome analysis (Kruft et al., 2001).

Mitochondria from cell culture were used to identify the general biochemical function of ETHE1. SDO activity was also measured in mitochondria prepared from rosette leaves of 8-week-old wild-type Arabidopsis plants grown under short-day conditions following the protocol described by Keech et al. (2005).

Proteomics

One-dimensional SDS-PAGE and protein-blot analysis were carried out following standard methods. Antibodies against purified 6× His-ETHE1 were produced by Biogenes, and antibodies against OAS (thiol) lyase, which recognize the three major isoforms of the protein, were used as published (Heeg et al., 2008).

Mitochondrial proteins from wild-type and *ethe1-1* cell culture were separated by two-dimensional IEF/SDS-PAGE as described by Hildebrandt et al. (2013) with some modifications: 0.5 mg of mitochondrial protein from each sample was solubilized by shaking in 450 μL of rehydration buffer (6 M urea, 2 M thiourea, 50 mM dithiothreitol, 2% [w/v] CHAPS, 5% [v/v] immobilized pH gradient buffer 3-11nl, 12 $\mu L\ mL^{-1}$ DeStreak reagent, and a trace of bromphenol blue) for 60 min at room temperature. IEF was carried out on Immobiline DryStrip gels (24 cm, nonlinear gradient pH 3–11) using the Ettan IPGphor 3 system (GE Healthcare). For the second dimension, the High Performance Electrophorese FlatTop Tower-System (Serva Electrophoresis) was used with precast Tris-Gly gels (12.5% polyacrylamide, 24 × 20 cm). Gel image analysis and protein identification by mass spectrometry were carried out as described by Hildebrandt et al. (2013). Briefly, spots were cut from the two-dimensional gels with a manual spot picker (Genetix), washed in 0.1 M ammonium bicarbonate, and dehydrated with acetonitrile. After tryptic digestion, peptides were extracted by successive incubation with 50% (v/v) acetonitrile plus 5% (v/v) formic acid, 50% (v/v) acetonitrile plus 1% (v/v) formic acid, 50% (v/v) acetonitrile plus 1% (v/v) formic acid, and 100% acetonitrile. Nano-HPLC electrospray ionization quadrupole time of flight mass spectrometry analyses were carried out using the Easy-nLC system (Proxeon) coupled to a micrOTOF-Q-II mass spectrometer (Bruker Daltonics). Liquid chromatography separation was achieved with a C18 reverse-phase column (Proxeon EASY-Column [length = 10 cm, i.d. = 75 μm]; ReproSil-Pur C18-AQ, 3 μm, 120 A) coupled to a Proxeon EASY-PreColumn (length = 2 cm, i.d. = 100 μm; ReproSil-Pur C18-AQ, 5 μm, 120 A) using an acetonitrile/formic acid gradient (Klodmann et al., 2011). Tandem mass spectrometry fragmentation was carried out automatically. Proteins were identified using the MASCOT search algorithm against The Arabidopsis Information Resource 10 (www.arabidopsis.org).

Miscellaneous Methods

A coexpression analysis based on a manually curated database of 40,000 microarrays was performed with Genevestigator (www.genevestigator.com; Hruz et al., 2008). Genes that are coregulated with *AT1G53580* under relevant

conditions were identified following a two-step workflow. First, experiments with a significant change ($P < 0.05$) of at least 1.5-fold in ETHE1 expression were selected using the perturbations tool. The 100 genes with the most similar expression patterns in these experiments were then identified with the coexpression tool using the Pearson correlation coefficient as the measure of similarity.

Protein was quantified using the Bio-Rad Protein Assay reagent, and iron was quantified using the colorimetric chelator ferene (Hennessy et al., 1984).

Supplemental Data

The following materials are available in the online version of this article.

Supplemental Figure S1. Purification, pH, and temperature optima of Arabidopsis and human ETHE1.

Supplemental Figure S2. Growth parameters of *ethe1-1* and wild-type rosettes under long-day conditions.

Supplemental Figure S3. Identification of proteins with altered abundance in mitochondria of *ethe1-1* compared with the wild type.

Supplemental Figure S4. Leaf senescence in wild-type and *ethe1-1* plants under long- and short-day growth conditions.

Supplemental Figure S5. Histochemical detection of ROS and reactive sulfur species in leaves of wild-type and *ethe1-1* plants.

Supplemental Table S1. Identification of substrates for recombinant ETHE1 and the SDO reaction in Arabidopsis mitochondria.

Supplemental Table S2. Identification of proteins with altered abundance in mitochondria of *ethe1-1* compared with the wild type.

Supplemental Table S3. Genes that are coexpressed with ETHE1 in Arabidopsis under relevant conditions.

Supplemental Table S4. Amino acid and GSH contents of wild-type and *ethe1-1* seeds at 4 to 5 d after pollination.

Supplemental Table S5. Metabolite contents of wild-type and *ethe1-1* rosette leaves under long- and short-day growth conditions as well as after extended darkness.

Supplemental Table S6. Contents of sulfite, thiosulfate, and sulfide in wild-type and *ethe1* mutant rosette leaves after 7 d of extended darkness.

ACKNOWLEDGMENTS

We thank Valeria Tiranti and Massimo Zeviani for providing the plasmid for the expression of human ETHE1, Christoph Peterhänsel and Steffanie Fromm for assistance with PCR experiments, Herbert Geyer and Jens-Peter Barth for taking care of the plants, Traud Winkelmann for support with the microscope, Mascha Brinkötter for taking part in histochemical ROS detection, and Lorna Jackson for optimizing the immunodetection of the ETHE1 protein. We thank the Metabolomics Core Technology Platform of the Excellence cluster CellNetworks (University of Heidelberg) for support with HPLC-based metabolite quantification.

Received March 17, 2014; accepted March 31, 2014; published April 1, 2014.

LITERATURE CITED

Alvarez C, Calo L, Romero LC, García I, Gotor C (2010) An *O*-acetylserine (thiol)lyase homolog with L-cysteine desulfhydrase activity regulates cysteine homeostasis in Arabidopsis. Plant Physiol **152:** 656–669

Álvarez C, García I, Moreno I, Pérez-Pérez ME, Crespo JL, Romero LC, Gotor C (2012) Cysteine-generated sulfide in the cytosol negatively regulates autophagy and modulates the transcriptional profile in *Arabidopsis*. Plant Cell **24:** 4621–4634

Araújo WL, Ishizaki K, Nunes-Nesi A, Larson TR, Tohge T, Krahnert I, Witt S, Obata T, Schauer N, Graham IA, et al (2010) Identification of the 2-hydroxyglutarate and isovaleryl-CoA dehydrogenases as alternative electron donors linking lysine catabolism to the electron transport chain of *Arabidopsis* mitochondria. Plant Cell **22:** 1549–1563

Araújo WL, Tohge T, Ishizaki K, Leaver CJ, Fernie AR (2011) Protein degradation: an alternative respiratory substrate for stressed plants. Trends Plant Sci **16:** 489–498

Baena-González E, Rolland F, Thevelein JM, Sheen J (2007) A central integrator of transcription networks in plant stress and energy signalling. Nature **448:** 938–942

Balk J, Pilon M (2011) Ancient and essential: the assembly of iron-sulfur clusters in plants. Trends Plant Sci **16:** 218–226

Birke H, Haas FH, De Kok LJ, Balk J, Wirtz M, Hell R (2012) Cysteine biosynthesis, in concert with a novel mechanism, contributes to sulfide detoxification in mitochondria of Arabidopsis thaliana. Biochem J **445:** 275–283

Boyes DC, Zayed AM, Ascenzi R, McCaskill AJ, Hoffman NE, Davis KR, Görlach J (2001) Growth stage-based phenotypic analysis of *Arabidopsis*: a model for high throughput functional genomics in plants. Plant Cell **13:** 1499–1510

Brychkova G, Grishkevich V, Fluhr R, Sagi M (2013) An essential role for tomato sulfite oxidase and enzymes of the sulfite network in maintaining leaf sulfite homeostasis. Plant Physiol **161:** 148–164

Buchner P, Stuiver CEE, Westerman S, Wirtz M, Hell R, Hawkesford MJ, De Kok LJ (2004) Regulation of sulfate uptake and expression of sulfate transporter genes in *Brassica oleracea* as affected by atmospheric H_2S and pedospheric sulfate nutrition. Plant Physiol **136:** 3396–3408

Bürstenbinder K, Waduwara I, Schoor S, Moffatt BA, Wirtz M, Minocha SC, Oppermann Y, Bouchereau A, Hell R, Sauter M (2010) Inhibition of 5′-methylthioadenosine metabolism in the Yang cycle alters polyamine levels, and impairs seedling growth and reproduction in Arabidopsis. Plant J **62:** 977–988

Di Meo I, Fagiolari G, Prelle A, Viscomi C, Zeviani M, Tiranti V (2011) Chronic exposure to sulfide causes accelerated degradation of cytochrome c oxidase in ethylmalonic encephalopathy. Antioxid Redox Signal **15:** 353–362

Dooley FD, Nair SP, Ward PD (2013) Increased growth and germination success in plants following hydrogen sulfide administration. PLoS ONE **8:** e62048

Fahnenstich H, Saigo M, Niessen M, Zanor MI, Andreo CS, Fernie AR, Drincovich MF, Flügge UI, Maurino VG (2007) Alteration of organic acid metabolism in Arabidopsis overexpressing the maize C4 NADP-malic enzyme causes accelerated senescence during extended darkness. Plant Physiol **145:** 640–652

García-Mata C, Lamattina L (2010) Hydrogen sulphide, a novel gasotransmitter involved in guard cell signalling. New Phytol **188:** 977–984

Geisler DA, Päpke C, Obata T, Nunes-Nesi A, Matthes A, Schneitz K, Maximova E, Araújo WL, Fernie AR, Persson S (2012) Downregulation of the δ-subunit reduces mitochondrial ATP synthase levels, alters respiration, and restricts growth and gametophyte development in *Arabidopsis*. Plant Cell **24:** 2792–2811

Giordano C, Viscomi C, Orlandi M, Papoff P, Spalice A, Burlina A, Di Meo I, Tiranti V, Leuzzi V, d'Amati G, et al (2012) Morphologic evidence of diffuse vascular damage in human and in the experimental model of ethylmalonic encephalopathy. J Inherit Metab Dis **35:** 451–458

Gu L, Jones AD, Last RL (2010) Broad connections in the Arabidopsis seed metabolic network revealed by metabolite profiling of an amino acid catabolism mutant. Plant J **61:** 579–590

Hatzfeld Y, Maruyama A, Schmidt A, Noji M, Ishizawa K, Saito K (2000) β-Cyanoalanine synthase is a mitochondrial cysteine synthase-like protein in spinach and Arabidopsis. Plant Physiol **123:** 1163–1171

Heeg C, Kruse C, Jost R, Gutensohn M, Ruppert T, Wirtz M, Hell R (2008) Analysis of the *Arabidopsis O*-acetylserine(thiol)lyase gene family demonstrates compartment-specific differences in the regulation of cysteine synthesis. Plant Cell **20:** 168–185

Hell R, Wirtz M (2011) Molecular biology, biochemistry and cellular physiology of cysteine metabolism in *Arabidopsis thaliana*. The Arabidopsis Book **9:** e0154, doi/10.1199/tab.0154

Hennessy DJ, Reid GR, Smith FE, Thompson SL (1984) Ferene: a new spectrophotometric reagent for iron. Can J Chem **62:** 721–724

Hildebrandt TM, Di Meo I, Zeviani M, Viscomi C, Braun HP (2013) Proteome adaptations in Ethe1-deficient mice indicate a role in lipid catabolism and cytoskeleton organization via post-translational protein modifications. Biosci Rep **33:** 575–584

Hildebrandt TM, Grieshaber MK (2008) Three enzymatic activities catalyze the oxidation of sulfide to thiosulfate in mammalian and invertebrate mitochondria. FEBS J **275:** 3352–3361

Holdorf MM, Owen HA, Lieber SR, Yuan L, Adams N, Dabney-Smith C, Makaroff CA (2012) Arabidopsis ETHE1 encodes a sulfur dioxygenase that is essential for embryo and endosperm development. Plant Physiol **160:** 226–236

Hruz T, Laule O, Szabo G, Wessendorp F, Bleuler S, Oertle L, Widmayer P, Gruissem W, Zimmermann P (2008) Genevestigator v3: a reference

expression database for the meta-analysis of transcriptomes. Adv Bioinformatics **2008:** 420747

Ishizaki K, Larson TR, Schauer N, Fernie AR, Graham IA, Leaver CJ (2005) The critical role of *Arabidopsis* electron-transfer flavoprotein:ubiquinone oxidoreductase during dark-induced starvation. Plant Cell **17:** 2587–2600

Ishizaki K, Schauer N, Larson TR, Graham IA, Fernie AR, Leaver CJ (2006) The mitochondrial electron transfer flavoprotein complex is essential for survival of Arabidopsis in extended darkness. Plant J **47:** 751–760

Izumi M, Hidema J, Makino A, Ishida H (2013) Autophagy contributes to nighttime energy availability for growth in Arabidopsis. Plant Physiol **161:** 1682–1693

Jander G, Norris SR, Joshi V, Fraga M, Rugg A, Yu S, Li L, Last RL (2004) Application of a high-throughput HPLC-MS/MS assay to Arabidopsis mutant screening: evidence that threonine aldolase plays a role in seed nutritional quality. Plant J **39:** 465–475

Jin Z, Shen J, Qiao Z, Yang G, Wang R, Pei Y (2011) Hydrogen sulfide improves drought resistance in *Arabidopsis thaliana*. Biochem Biophys Res Commun **414:** 481–486

Jin Z, Xue S, Luo Y, Tian B, Fang H, Li H, Pei Y (2013) Hydrogen sulfide interacting with abscisic acid in stomatal regulation responses to drought stress in Arabidopsis. Plant Physiol Biochem **62:** 41–46

Kabil O, Banerjee R (2012) Characterization of patient mutations in human persulfide dioxygenase (ETHE1) involved in H_2S catabolism. J Biol Chem **287:** 44561–44567

Keech O, Dizengremel P, Gardeström P (2005) Preparation of leaf mitochondria from Arabidopsis thaliana. Physiol Plant **124:** 403–409

Klodmann J, Senkler M, Rode C, Braun HP (2011) Defining the protein complex proteome of plant mitochondria. Plant Physiol **157:** 587–598

Kruft V, Eubel H, Jänsch L, Werhahn W, Braun HP (2001) Proteomic approach to identify novel mitochondrial proteins in Arabidopsis. Plant Physiol **127:** 1694–1710

Lang C, Popko J, Wirtz M, Hell R, Herschbach C, Kreuzwieser J, Rennenberg H, Mendel RR, Hänsch R (2007) Sulphite oxidase as key enzyme for protecting plants against sulphur dioxide. Plant Cell Environ **30:** 447–455

Li F, Vierstra RD (2012) Autophagy: a multifaceted intracellular system for bulk and selective recycling. Trends Plant Sci **17:** 526–537

Li ZG, Gong M, Xie H, Yang L, Li J (2012) Hydrogen sulfide donor sodium hydrosulfide-induced heat tolerance in tobacco (*Nicotiana tabacum* L) suspension cultured cells and involvement of Ca^{2+} and calmodulin. Plant Sci **185-186:** 185–189

Mao G, Wang R, Guan Y, Liu Y, Zhang S (2011) Sulfurtransferases 1 and 2 play essential roles in embryo and seed development in *Arabidopsis thaliana*. J Biol Chem **286:** 7548–7557

May MJ, Leaver CJ (1993) Oxidative stimulation of glutathione synthesis in *Arabidopsis thaliana* suspension cultures. Plant Physiol **103:** 621–627

McCoy JG, Bingman CA, Bitto E, Holdorf MM, Makaroff CA, Phillips GN Jr (2006) Structure of an ETHE1-like protein from *Arabidopsis thaliana*. Acta Crystallogr D Biol Crystallogr **62:** 964–970

Niessen M, Krause K, Horst I, Staebler N, Klaus S, Gaertner S, Kebeish R, Araujo WL, Fernie AR, Peterhänsel C (2012) Two alanine aminotransferases link mitochondrial glycolate oxidation to the major photorespiratory pathway in Arabidopsis and rice. J Exp Bot **63:** 2705–2716

Riemenschneider A, Wegele R, Schmidt A, Papenbrock J (2005) Isolation and characterization of a D-cysteine desulfhydrase protein from *Arabidopsis thaliana*. FEBS J **272:** 1291–1304

Robison MM, Ling X, Smid MPL, Zarei A, Wolyn DJ (2009) Antisense expression of mitochondrial ATP synthase subunits OSCP (ATP5) and γ (ATP3) alters leaf morphology, metabolism and gene expression in Arabidopsis. Plant Cell Physiol **50:** 1840–1850

Rohwerder T, Sand W (2003) The sulfane sulfur of persulfides is the actual substrate of the sulfur-oxidizing enzymes from *Acidithiobacillus* and *Acidiphilium* spp. Microbiology **149:** 1699–1710

Shaw L, Engel PC (1987) CoA-persulphide: a possible in vivo inhibitor of mammalian short-chain acyl-CoA dehydrogenase. Biochim Biophys Acta **919:** 171–174

Sunderhaus S, Dudkina NV, Jänsch L, Klodmann J, Heinemeyer J, Perales M, Zabaleta E, Boekema EJ, Braun HP (2006) Carbonic anhydrase subunits form a matrix-exposed domain attached to the membrane arm of mitochondrial complex I in plants. J Biol Chem **281:** 6482–6488

Szal B, Dąbrowska Z, Malmberg G, Gardeström P, Rychter AM (2008) Changes in energy status of leaf cells as a consequence of mitochondrial genome rearrangement. Planta **227:** 697–706

Taylor NL, Heazlewood JL, Day DA, Millar AH (2004) Lipoic acid-dependent oxidative catabolism of α-keto acids in mitochondria provides evidence for branched-chain amino acid catabolism in Arabidopsis. Plant Physiol **134:** 838–848

Thordal-Christensen H, Zhang Z, Wei Y, Collinge DB (1997) Subcellular localization of H_2O_2 in plants: H_2O_2 accumulation in papillae and hypersensitive response during the barley-powdery mildew interaction. Plant J **11:** 1187–1194

Tiranti V, D'Adamo P, Briem E, Ferrari G, Mineri R, Lamantea E, Mandel H, Balestri P, Garcia-Silva MT, Vollmer B, et al (2004) Ethylmalonic encephalopathy is caused by mutations in ETHE1, a gene encoding a mitochondrial matrix protein. Am J Hum Genet **74:** 239–252

Tiranti V, Viscomi C, Hildebrandt T, Di Meo I, Mineri R, Tiveron C, Levitt MD, Prelle A, Fagiolari G, Rimoldi M, et al (2009) Loss of ETHE1, a mitochondrial dioxygenase, causes fatal sulfide toxicity in ethylmalonic encephalopathy. Nat Med **15:** 200–205

van Hoewyk D, Pilon M, Pilon-Smits EA (2008) The functions of NifS-like proteins in plant sulfur and selenium metabolism. Plant Sci **174:** 117–123

Werhahn W, Niemeyer A, Jänsch L, Kruft V, Schmitz UK, Braun HP (2001) Purification and characterization of the preprotein translocase of the outer mitochondrial membrane from Arabidopsis: identification of multiple forms of TOM20. Plant Physiol **125:** 943–954

Wirtz M, Hell R (2003) Production of cysteine for bacterial and plant biotechnology: application of cysteine feedback-insensitive isoforms of serine acetyltransferase. Amino Acids **24:** 195–203

Zhang H, Hu LY, Hu KD, He YD, Wang SH, Luo JP (2008) Hydrogen sulfide promotes wheat seed germination and alleviates oxidative damage against copper stress. J Integr Plant Biol **50:** 1518–1529

Zhang H, Tan ZQ, Hu LY, Wang SH, Luo JP, Jones RL (2010) Hydrogen sulfide alleviates aluminum toxicity in germinating wheat seedlings. J Integr Plant Biol **52:** 556–567

Zhu X, Tang G, Granier F, Bouchez D, Galili G (2001) A T-DNA insertion knockout of the bifunctional lysine-ketoglutarate reductase/saccharopine dehydrogenase gene elevates lysine levels in Arabidopsis seeds. Plant Physiol **126:** 1539–1545